Brain Pathology ISSN 1015-6305

RESEARCH ARTICLE

Upregulation of Shiga Toxin Receptor CD77/Gb3 and Interleukin-1β Expression in the Brain of EHEC Patients with Hemolytic Uremic Syndrome and Neurologic Symptoms

Christian Hagel[1]; Susanne Krasemann[1]; Judith Löffler[1]; Klaus Püschel[2]; Tim Magnus[3]; Markus Glatzel[1]

[1] Institute of Neuropathology, [2] Department of Legal Medicine, [3] Department of Neurology, University Medical Center Hamburg-Eppendorf, Hamburg, Germany.

Keywords
CD77/Gb3, enterohemorrhagic *Escherichia coli*, hemolytic uremic syndrome, microglia, neuropathology, vasculature.

Corresponding author:
Christian Hagel, MD, Institute of Neuropathology, University Medical Center Hamburg-Eppendorf, Martinistr. 52, D-20246 Hamburg, Germany (E-mail: *hagel@uke.de*)

Received 10 February 2014
Accepted 18 June 2014
Published Online Article Accepted 2 July 2014

doi:10.1111/bpa.12166

Abstract

In 2011, a large outbreak of Shiga toxin-producing enterohemorrhagic *Escherichia coli* (EHEC) infections occurred in northern Germany, which mainly affected adults. Out of 3842 patients, 104 experienced a complicated course comprising hemolytic uremic syndrome and neurological complications, including cognitive impairment, aphasia, seizures and coma. T2 hyperintensities on magnet resonance imaging (MRI) bilateral in the thalami and in the dorsal pons were found suggestive of a metabolic toxic effect. Five of the 104 patients died because of toxic heart failure. In the present study, the post-mortem neuropathological findings of the five EHEC patients are described. Histological investigation of 13 brain regions (frontal, temporal, occipital cortex, corpora mammillaria, thalamus, frontal operculum, corona radiata, gyrus angularis, pons, medulla oblongata, cerebellar vermis and cerebellar hemisphere) showed no thrombosis, ischemic changes or fresh infarctions. Further, no changes were found in electron microscopy. In comparison with five age-matched controls, slightly increased activation of microglia and a higher neuronal expression of interleukin-1β and of Shiga toxin receptor CD77/globotriaosylceramide 3 was observed. The findings were confirmed by Western blot analyses. It is suggested that CD77/globotriaosylceramide upregulation may be a consequence to Shiga toxin exposure, whereas increased interleukin-1β expression may point to activation of inflammatory cascades.

INTRODUCTION

Patients infected with Shiga toxin (Stx)-expressing *Escherichia coli* (STEC) may develop a hemorrhagic colitis and hemolytic uremic syndrome (HUS). Both complications have been attributed to Stx-induced microvascular injury resulting in thrombosis, as Stx binds to digalactosyl receptors on microvascular endothelial cells in gut, kidney and brain.

The outbreak of enterohemorrhagic *Escherichia coli* (EHEC) infections in northern Germany in spring 2011 was caused by the Stx2 variant O104:H4, a strain with enteroaggregative properties (19). In contrast to previous series that mostly involved children and always struck less than 100 individuals, 3842 individuals were affected and 90% of these were adults (6). In 104 of the patients, neurological complications developed comprising cognitive impairment, aphasia, seizures and coma (12). All patients of this subgroup suffered from a complicated course of the disease, including HUS. The onset of neurological symptoms was paralleled—although not regularly—by a rise of creatinine and urea. The most frequently involved brain regions in magnet resonance imaging (MRI) in 51 patients were thalamus (39%), pons (35%), the centrum semiovale and the splenium of the corpus callosum (33%). Bilateral symmetric T2 hyperintense lesions of the thalami and dorsal pons characterized by restricted diffusion were found suggestive of a metabolic toxic effect (11).

Hitherto, the pathophysiology of neurological symptoms in EHEC infection remains unclear. However, a number of hypotheses have been put forward, mainly based on data from cell culture and animal studies. All of these hypotheses propose Shiga toxin receptor CD77/globotriaosylceramide 3 (CD77/Gb3) mediated effects including (i) endothelial damage with subsequent thrombosis; (ii) activation of inflammatory pathways; or (iii) direct cytotoxicity (9).

In the present study, we investigated the neuropathological features of five EHEC patients with neurological symptoms and describe a correlation between EHEC with neurological complications and increased levels of Shiga toxin receptor CD77/Gb3 in neurons paralleled by microglia activation and increased interleukin-1β (IL-1β) expression providing novel clues to EHEC pathophysiology.

MATERIALS AND METHODS

Patients

The characteristics of the five patients and the five controls are depicted in Table 1. Detailed neurological and clinical chemistry data on the course of the disease were available for four patients and MRI scans were performed in two patients (Table 2).

Tissue specimens

Prior to fixation in formalin, samples from the frontal cortex were taken from case #2 and #4 and deep-frozen at −80°C. After fixation in formalin for 3 weeks, the brains were investigated macroscopically and samples were taken for histological examination from the following regions: frontal, temporal and occipital cortex, corpora mammillaria, thalamus, frontal operculum, corona radiata, gyrus angularis, pons, medulla oblongata, cerebellar vermis and cerebellar hemisphere.

The controls comprised samples from the following regions: frontal, temporal and occipital cortex, corpora mammillaria, thalamus, pons, medulla oblongata, cerebellar vermis and cerebellar hemisphere. For histological examination, the specimens were dehydrated, paraffin embedded and 4-µm-thick sections were cut and stained with hematoxylin and eosin (H&E), Periodic acid Schiff (PAS), Elastica van Gieson and Turnbull.

Immunohistochemistry

For immunohistochemical labeling, 4-µm-thick sections of the thalamus and brain stem were pretreated and incubated with primary antibodies, as indicated in Table 3, in an automated stainer (Ventana Medical Systems, Tucson, AZ, USA) according to standard protocols. Bound antibodies were detected by the peroxidase method using diaminobenzidine as chromogen (Ultraview DAB, 760-500, Ventana Medical Systems). The number of CD77- and VCAM-1-positive vessels was counted in a representative area of 9 mm^2 using a 40× objective (0.19 mm^2/field). Only vessels with an identifiable lumen were included. Activated caspase 3 was assessed by counting all positive nuclei in a representative area of 1 cm^2 using a 40× objective (samples from fresh infarctions served as positive controls). All other markers were evaluated semiquantitatively according to the following criteria: no staining = 0, weak staining = 1, moderate staining = 2, strong staining = 3.

Immunofluorescence analysis

Deep-frozen brain samples were cut into 8-µm sections and fixed in cold acetone or methanol. After washing, permeabilization using 0.05% Triton X-100 (0.2% for IL-1β) and blocking (protein-free T20 blocking buffer, Thermo Scientific, Rockford, IL, USA), slides were incubated with primary antibody for CD77/Gb3 (1:50, 4°C overnight; see Table 3) or IL-1β (1:100, 4°C overnight; see Table 3) washed, incubated with the FITC-coupled (BioLegend, 408905, San Diego, CA, USA; 1 h, room temperature) or Alexa555-coupled secondary antibody (Life Technologies/Molecular Probes, A31572, Darmstadt, Germany; 1 h, room temperature), washed again and mounted with DAPI-Fluoromount G (SouthernBiotech, 0100-20, Birmingham, AL, USA). Analysis was performed using a TCS SP5 confocal microscope (Leica, Wetzlar, Germany) and LAS AF Lite software (Leica). For quantitative assessment of IL1-β fluorescence ImageJ software (NIH, Version 1.47, Bethesda, MD, USA) was used. A representative area of the frontal cortex of EHEC and control patients was chosen for analysis, and the cytoplasm of 50 neurons was manually marked and the fluorescence intensity related to the area was measured.

Electron microscopy

For electron microscopy, paraffin-embedded samples from the thalamus and brain stem of patient nos. 2 and 4 were de-waxed and embedded in Epon 812 (Serva). After polymerization of the resin, semithin sections of 1 µm were cut and stained with toluidine blue.

Table 1. Data of enterohemorrhagic *Escherichia coli* (EHEC) patients and controls.
Abbreviations: f = female; m = male; n.d. = not determined; HUS = hemolytic uremic syndrome, d = days; neuro = neurological symptoms.

Patient	Age	Gender	Underlying disease	Acute illness/cause of death	Post-mortem time (d)	Diarrhea to HUS (d)	HUS to neuro (d)	Neuro to death (d)	Diarrhea to death (d)
1	87	f	Cardiovascular/diabetes	HUS/toxic heart failure	4	7	1	4	12
2	81	f	Cardiovascular/diabetes	HUS/toxic heart failure	1	14	1	2	17
3	83	m	Cardiovascular/diabetes	HUS/toxic heart failure	—	14	0	5	19
4	66	f	Cardiovascular/diabetes	HUS/toxic heart failure	2	4	4	13	21
5	70	m	Cardiovascular/diabetes	HUS/toxic heart failure	2	3	9	12	24
6	74	f	Myelodysplastic syndrome	Pneumonia	4				
7	70	f	Colon carcinoma	Septic shock	—				
8	73	m	Arterial hypertension, diabetes	Heart failure	5				
9	78	m	Colon carcinoma	Pulmonary embolism	3				
10	91	f	Fracture of the neck of the femur	Peritonitis	3				

Mean post-mortem time in EHEC cases: 2.25 days.
Mean post-mortem time in controls: 3.75 days.

Table 2. Clinical course of enterohemorrhagic *Escherichia coli* (EHEC) infection in patients 2–5 (no data for patient 1). Symptoms that were not detected or not assessable: headache, distal paresis, cranial nerve palsy; n.a. = not assessable; n.d. = not determined; EEG1 = general EEG changes; EEG4 = combination of general and focal EEG changes; MRI0 = no changes; MRI5 = combination of cortical, subcortical, thalamo-pontin and callosal MRI changes; modified Rankin scale: 0—no symptoms, 1—no significant disability (able to carry out all usual activities, despite some symptoms), 2—slight disability (able to look after own affairs without assistance, but unable to carry out all previous activities), 3—moderate disability (requires some help, but able to walk unassisted), 4—moderately severe disability (unable to attend to own bodily needs without assistance, and unable to walk unassisted), 5—severe disability (requires constant nursing care and attention, bedridden, incontinent), 6—dead; Hb, minimal hemoglobin level; leucocyte, maximal leucocyte counts; thrombo, minimal thrombocyte counts; GFR, minimal glomerular filtration rate (60 or higher = 60); CRP = maximal C-reactive protein levels (below 5 = 0); LDH = maximal levels of lactate dehydrogenase.

Patient No.	Week	Organic brain syndrome	Aphasia	Seizures	Other neurological symptoms	Intubation	Complications	MRI/EEG changes	Modified rankin scale	Min. Hb (g/dL)	Max. leucocyte (10^9/L)	Min. thrombo. (10^9/L)	Max. urea (mg/dL)	Max. creatinine (mg/dL)	Min. GFR (mL/minute)	Max. CRP (mg/L)	Max. LDH (U/L)
2	1	Severe	severe	No	No	No	None	n.d.	0	n.d.	n.d.	n.d.	n.d.	n.d.	n.d.	n.d.	n.d.
	2	Severe	severe	No	No	No	None	EEG4	5	11	12	204	26	2		7	427
	3	Severe	severe	Yes	No	No	Death	n.d.	6	10	23	69	52	2	24	8	684
3	1	None	None	No	No	No	None	n.d.	5	n.d.	n.d.	n.d.	n.d.	n.d.	n.d.	n.d.	n.d.
	2	Mild	Mild	No	Yes	No	None	n.d.	5	10	12	234	46	3	n.d.	223	306
	3	n.a.	n.a.	Yes	Yes	Yes	Death	n.d.	6	10	47	34	57	5	13	205	1 527
4	1	None	None	No	No	No	None	n.d.	1	11	26	34	57	3	n.d.	266	1 399
	2	Severe	None	No	No	Yes	Sepsis	n.d.	5	6	56	31	81	4	13	229	1 685
	3	n.a.	n.a.	No	No	Yes	Sepsis	n.d.	5	6	18	44	57	3	20	255	4 935
	4	n.a.	n.a.	No	No	Yes	Death	MRI5	6	10	17	44	19	1	44	33	13 559
5	1	None	None	No	No	No	None	n.d.	2	16	20	232	42	1	60	204	314
	2	Mild	None	No	No	No	None	MRI0, EEG1	2	12	19	53	67	2	30	145	684
	3	Mild	None	No	No	No	None	n.d.	4	12	28	135	76	3	20	184	567
	4	None	None	No	No	No	Death	n.d.	6	12	25	199	94	4	17	135	453

Table 3. Primary antibodies.
Abbreviations: GFAP = glial fibrillary acidic protein; IBA-1 = ionized calcium-binding adapter molecule 1; IL-1β = interleukin 1β; LAMP-1 = lysosomal-associated membrane protein-1; LCA, leukocyte common antigen; MAP2c = microtubule-associated protein 2c; TNF-α = tumor necrosis factor-α; VCAM = vascular cell adhesion molecule-1; VEGF = vascular endothelial growth factor.

Antigen	Antibody supplier	City	Country	Order No.	Pretreatment	Buffer	Dilution
von Willebrand factor	Dako	Hamburg	Germany	A0 082	CC1st	Citrate buffer	1:1500
VEGF	Santa Cruz	Santa Cruz	USA	Sc7269	CC1st	Citrate buffer	1:1000
Angiopoietin-1	Abcam	UK	Cambridge	ab133425	CC2st	EDTA	1:100
Zonula-occludens-1	Invitrogen	Camarillo	USA	40–2300	CC1st	Citrate buffer	1:50
VCAM-1	antibodies-online.de	Aachen	Germany	ABIN574087	CC1st	Citrate buffer	1:200
CD34	Dako	Hamburg	Germany	M7165	None		1:100
GFAP	Dako	Hamburg	Germany	M0761	CC1st	Citrate buffer	1:200
Vimentin	Dako	Hamburg	Germany	M0725	CC1st	Citrate buffer	1:200
Nestin	Millipore	Billerica	USA	MAB353	CC1st	Citrate buffer	1:50
MAP2c	Sigma-Aldrich	St. Louis	USA	M4403	CC1st	Citrate buffer	1:3000
LCA	Dako	Hamburg	Germany	M0701	None	—	1:400
IBA-1	Wako	Osaka	Japan	019–19741	CC1st	Citrate buffer	1:200
HLA-DR	Dako	Hamburg	Germany	M0775	CC1st	Citrate buffer	1:200
TNF-α	Abcam	UK	Cambridge	ab1793	CC1st	Citrate buffer	1:20
IL-1β (cryo)	Abcam	UK	Cambridge	ab2105	None	—	1:100
LAMP-1	Santa Cruz	Santa Cruz	USA	Sc-20011	CC1m	Citrate buffer	1:100
CD77/Gb3	Beckman Coulter	Marseille	France	PN IM0175	Protease	—	1:20
Caspase 3	R&D Systems	—	USA	AF835	CC1st	Citrate buffer	1:100

Appropriate specimens were further processed for electron microscopy by cutting 60- to 80-nm-thick sections, which were contrasted with uranyl-acetate and lead solution.

Immunoblotting

For Western blot analysis, deep-frozen cortex brain samples from patients and controls were homogenized (FastPrep FP120, Qbiogene, Illkirch, France) in a buffer (150 mM NaCl, 1% NP-40, 0.5% DOC, 0.1% SDS, 50 mM Tris–HCl, pH 8.0) containing protease inhibitor. Samples were analyzed by sodium dodecyl sulfate–polyacrylamide gel electrophoresis (SDS-PAGE) (Mini-Protean TGX Any kD, Bio-Rad, Munich, Germany) and transferred to polyvinylidene fluoride (PVDF) membranes (BioRad, Hercules, FL, USA). Primary antibodies used for detection were ionized calcium-binding adapter molecule 1 (IBA-1, 1:1,000, see Table 2), heat shock protein 70 (Hsp70, 1:100, 610607, BD Biosciences, Heidelberg, Germany), IL-1β (1:200, ab2105, Abcam, Cambridge, UK), CD77/Gb3 (1:200, see Table 2), β-actin (1:5000, A5060, Sigma, St. Louis, MO, USA), as well as the respective anti-mouse, anti-rabbit and anti-rat secondary antibodies (1:10 000). Signals were detected using ECL or ECL femto reagent (Thermo Scientific).

Statistical analysis

All statistical analyses were calculated using the SSPS for Windows software release 20 (IBM Corp., Armonk, NY, USA). Levels of significance were computed according to the Mann–Whitney *U*–Wilcoxon rank-sum test for ordinal-scaled data and with Student's *t*-test for metrical data. The median values and 95% confidence interval (95% CI) and level of significance were computed. Kendall's tau was calculated to analyze the association between the intensity of immunohistochemical markers. All statistical analyses were intended to be rather exploratory than confirmatory. All P-values < 0.05, two-tailed, were considered statistically significant.

RESULTS

Macroscopic investigation of the brain did not reveal changes specifically related to EHEC or HUS. A mild (patient nos. 2, 3, 5) or moderate (patient no. 4) indentation of the lower vermis was the only sign of brain swelling. In case 3, an old thrombotic infarction in the territories of the left middle cerebral artery and the middle branch of the inferior posterior cerebellar artery was observed. Additionally, an unruptured aneurysm of the communicating anterior artery was detected in this patient.

To asses putative pathways involved in neuronal distress, tissue samples were examined on the histological and ultrastructural level as well as by immunoblotting for changes of the vasculature and the brain parenchyma, for signs of apoptosis, for activation of the immune system and for expression of the Shiga toxin receptor CD77/Gb3.

Upon histological examination, no signs of edema were detected; however, case #5 showed a spongy texture of the tissue in the pons and in addition fresh hypoxic–ischemic alterations in the hippocampus. This patient was reanimated some hours before he died. In patient no. 3, hemosiderin deposits were observed in the thalamus in the vicinity of the old infarction in the Turnbull stain. Concerning the vasculature and the brain parenchyma, no thrombosis, diffuse or circumscribed ischemic changes, fresh infarctions or signs of microhemorrhage were observed in H&E and Turnbull staining (Figure 1A,B). In addition, immunohistochemistry of von Willebrand factor (vWF), zonula-occludens-1 (ZO-1) and CD34 demonstrated expression typically restricted to endothelial cells

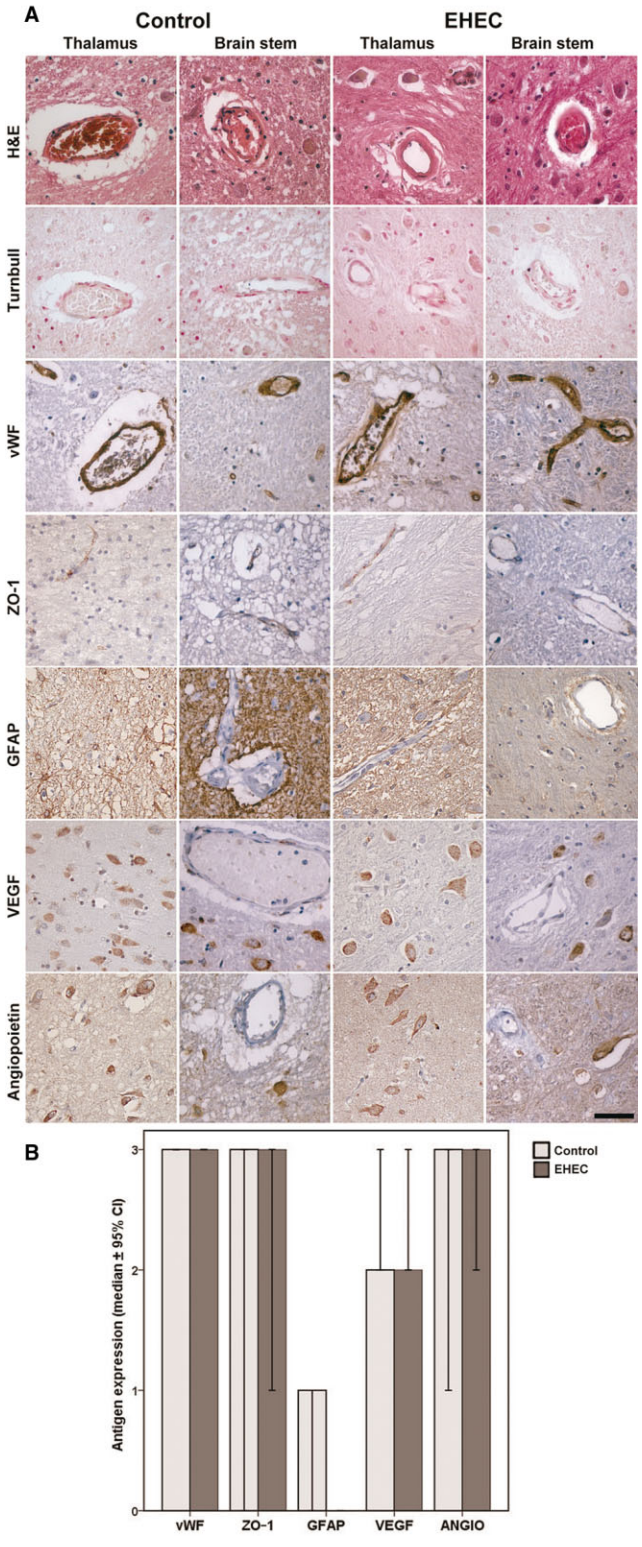

Figure 1. Vasculature-related parameters in adult enterohemorrhagic *Escherichia coli* (EHEC) patients and controls. A. Upper row: small vessels in thalamus and brain stem of controls and EHEC brains showing some congestion but no thrombotic microangiopathy; second row: no signs of previous microbleeds in Turnbull stain; third row: regular endothelial expression of von Willebrand Factor (vWF) without evidence for vWF multimers; forth row: zonulo-occludens-1 (ZO-1) immunohistochemistry showing regular expression in controls and EHEC cases; fifth row: normal glial fibrillary acidic protein (GFAP) expression in controls and EHEC cases; sixth row: normal vascular endothelial growth factor (VEGF) expression in neurons in both, controls and EHEC cases; seventh row: normal angiopoietin-1 expression in neurons of controls and EHEC patients; all microphotographs from case #2 and #6, respectively; counter stain for all immunohistochemical samples hemalum. Scale bar: 50 μm. B. Semiquantitative evaluation of vasculature related antigens expressed in controls and EHEC patients, median values ± 95% confidence intervals.

with no differences between controls and EHEC patients (Figure 1A,B; Supporting Information Figure S1). Antibodies against vascular cell adhesion molecule-1 (VCAM-1) showed strong binding to fiber tracts, diffusely labeled the neuropil and, to a varying degree, endothelia. In the latter, it was detected more frequently in EHEC cases than in controls (mean percentage of labeled vessels in the thalamus of controls: 17.2% vs. 55.0% in EHEC cases, in the brain stem of controls 24.5% vs. 28.6% in EHEC cases; Supporting Information Figure S1). However, this difference was statistically not significant because of a high standard deviation, which, in turn, resulted from difficulties in differentiating the vessels from the adjacent neuropil. Neurons stained positive for vascular endothelial growth factor (VEGF), angiopoietin-1 and microtubule-associated protein 2c (MAP2c) with no discernible differences between groups, whereas all cases but one control were negative for nestin labeling (Figure 1A,B; Supporting Information Figure S1). Astrocytes did not express vimentin (Supporting Information Figure S1), but glial fibrillary acidic protein (GFAP) labeling demonstrated patchy astrogliosis predominantly in the thalamus around vessels in both groups (Figure 1A,B).

Integrity of physiological brain structures was also demonstrated on the electron microscopic level. Post-mortem tissue was relatively well preserved and the organelles of neurons and glia as well as endothelial cells showed no specific changes, in particular the nuclei, the rough endoplasmic reticulum and the mitochondria appeared unaltered (Figure 2).

Further, there was no indication for *apoptosis*, neither as karyorrhexia in standard H&E stains nor in quantitative evaluation of nuclear caspase-3 expression, which was completely negative in EHEC and control samples (no positive nuclei at all)—in contrast to positive controls of fresh infarctions (1140 and 1426 mainly endothelial nuclei in cases A and B, respectively; 71 neuronal nuclei in case C in an area of 1 cm^2 each).

Activation of *inflammatory cascades* such as increased IL-1β production has previously been demonstrated in macrophages in EHEC infection (20). Thus, we investigated key components of neuroinflammation such as tumor necrosis factor α (TNF-α) and IL-1β in EHEC patients and controls. Leukocyte antigen (LCA) labeling only demonstrated few scattered lymphocytes predominantly around vessels in EHEC cases and controls, and TNF-α showed slight diffuse staining of the tissue matrix and within neurons in both groups (Figure 3). However, demonstration of

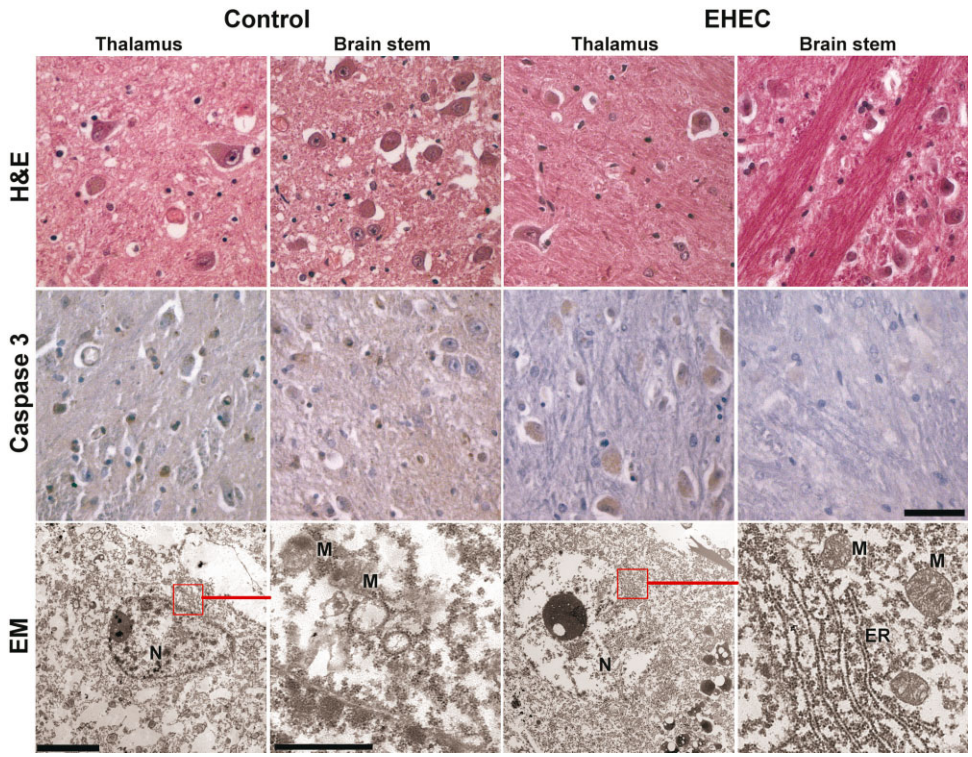

Figure 2. Lack of apoptosis and normal ultrastructure in adult enterohemorrhagic *Escherichia coli* (EHEC) patients and controls. Upper row: representative samples of thalamus and brain stem of EHEC patients and controls depicting neurons with normal morphology, H&E; middle row: negative labeling with antibodies against activated caspase 3, counter stain hemalum, all microphotographs in the first two rows from case #2 and #6, respectively; scale bar for first two rows, 50 µm; lower row: normal ultrastructure of neurons in post-mortem brain tissue showing intact nuclei (N), mitochondria (M) and endoplasmic reticulum (ER), scale bar in left picture 5 µm, scale bar in left close up view 1 µm, scale bars apply accordingly to the EHEC sample on the right.

IBA-1 and major histocompatibility complex II (MHC II, HLA-DR/DP/DQ-antibodies) revealed a slightly increased activation of microglia in EHEC patients (median level 2 vs. level 3 for IBA-1 and 0 vs. 1 for MHC II, respectively) with considerable variation between cases. Quantitative analysis of immunofluorescence staining of IL-1β revealed an increased labeling of neurons in EHEC patients that reached statistical significance (arbitrary units for fluorescence intensity, mean values 12.8 vs. 20.9, $P < 0.0001$; Figure 3A,C).

Development of HUS essentially depends on the expression of the Shiga toxin receptor CD77/Gb3 (13). We assessed the expression levels of CD77/Gb3 by immunohistochemistry. This showed an upregulation of Shiga toxin receptor in the neurons of EHEC patients compared with controls, although CD77 positivity varied and some controls also showed strong labeling (median level of 3 in EHEC vs. 1 in controls, $P = 0.023$, Mann–Whitney test; calculation for thalamus samples alone $P = 0.056$, brain stem samples alone $P = 0.222$; Table 4 and Figure 4A,B). Counts of vessels with CD77-positive endothelia did not differ between EHEC and control patients (Figure 4C,D). However, CD77 expression in the vasculature was weakly associated with VEGF expression when samples were pooled (EHEC patients plus controls, calculation for thalamus samples alone $P = 0.036$, brain stem samples alone $P = 0.046$, all samples $P = 0.005$, Kendall-tau-b; Table 4, Figure 4C,D).

Labeling of lysosomal-associated membrane protein-1 (LAMP-1) resulted in strong staining of vasculature and neurons and a light diffuse staining of the neuropil without differences in EHEC cases and controls (Supporting Information Figure S1).

In accordance with immunohistochemistry-based assessment of CD77 expression, we found significantly increased levels of CD77 in Western blot analyses of frontal cortex of EHEC patients 2 and 4 compared with control tissue (Figure 5). Further, and in agreement with immunohistochemical labeling of tissue from thalamus and brain stem, higher levels of IBA-1 and IL-1β could be demonstrated in Western blot analyses, whereas Hsp70 was not upregulated (Figure 5).

Explorative statistical analysis did not reveal any possible association between neurological symptoms, MRI findings, clinical chemistry data and the neuropathological alterations in patients 2–5.

DISCUSSION

In EHEC infection, a complicated course of the disease may lead to HUS and to neurological symptoms, some of which may persist for a long time after the acute stage of the disease (12, 17). In the 2011 EHEC outbreak in Germany, 3 pediatric patients out of 23 with acute neurological symptoms still had problems after 4 months consisting of fine motor deficits (n = 2) or deficits in

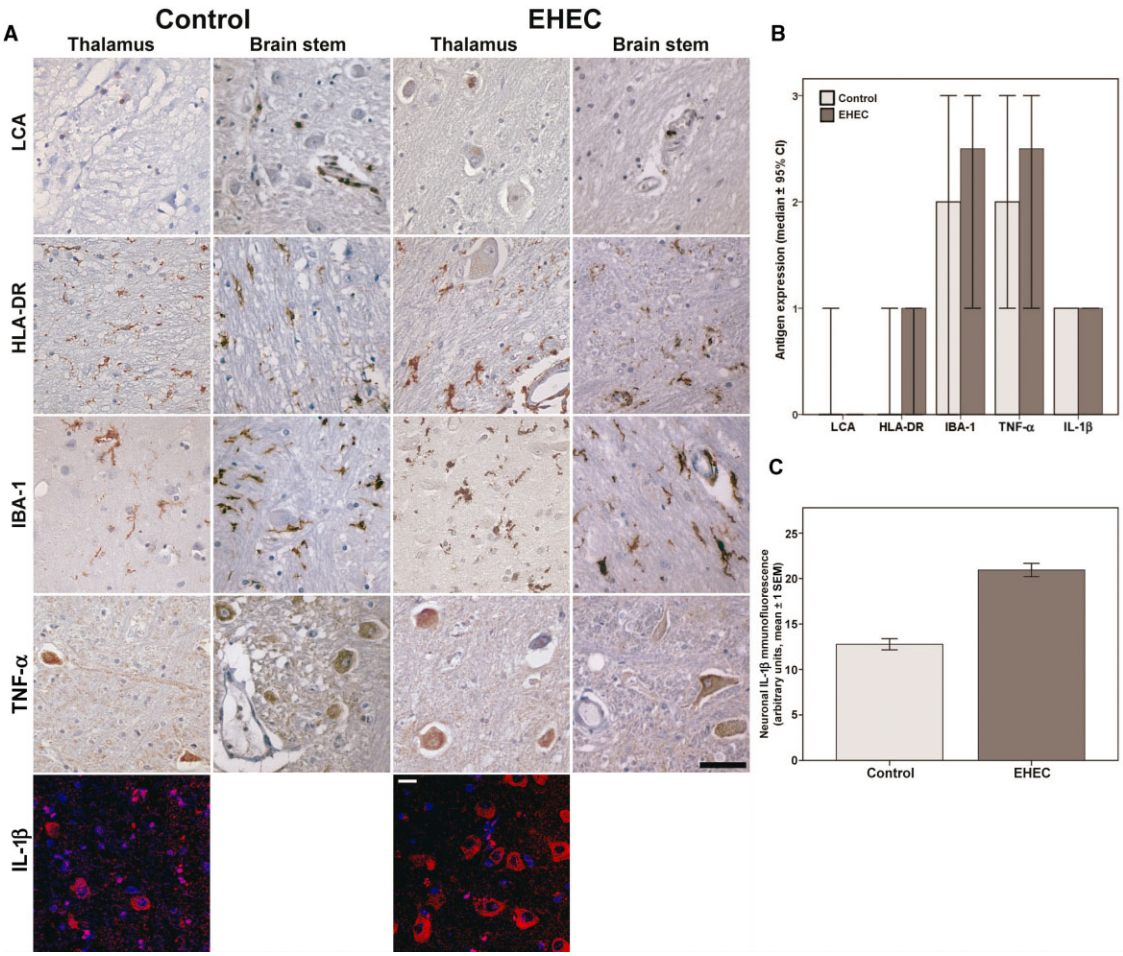

Figure 3. Inflammation-related parameters in the brain of adult enterohemorrhagic *Escherichia coli* (EHEC) patients and controls. A. First row: representative samples of thalamus and brain stem of EHEC patients and controls showing few scattered lymphocytes in both groups by labeling with antibodies against common leukocyte antigen (LCA); second and third row: labeling of major histocompatibility complex II (HLA-DR) and IBA-1 demonstrating slightly increased ramified microglia cells in EHEC patients; fourth row; no differences in TNF-α expression in both groups; all microphotographs in the first five rows from case #2 and #6, respectively; scale bar 50 μm applies for the first five rows, counterstain hemalum; fifth row: increased IL-1β expression in cortical neurons in EHEC patients in immunofluorescence, nuclear staining with DAPI. Scale bar: 10 μm. B. Semiquantitative evaluation of expression of inflammation associated antigens in controls and EHEC patients, median values ± 95% confidence intervals. C. Quantification of cytoplasmic IL-1β-immunofluorescence in 50 neurons of the frontal cortex in a control and an EHEC brain in relation to the area, arbitrary units, mean values ± 1 standard error of the mean, $P < 0.0001$.

concentration (n = 1) (10). Of the 104 adults with acute neurological symptoms, there were 3 patients with neurological sequelae comprising cortical blindness, aphasia and cognitive deficits (12). In a previous report on 52 pediatric cases with HUS and neurological symptoms, 13 out of 43 surviving children showed several neurologic deficits ranging from paresia (n = 3), hemiparesis (n = 2), epilepsy (n = 2) and developmental delay (n = 1) to severe disabilities (n = 5) (17). During the German EHEC outbreak, 1 out of 23 pediatric patients with neurologic symptoms died (10) and 5 out of 104 adults deceased (12). In the study reported by Nathanson *et al* (17), there were nine deaths. Autopsies of 32 brains of children who died in the course of diarrhea-associated HUS revealed thrombotic microangiopathy in 11 patients, which was located in the choroid plexus in 8 patients. In addition, intracranial hemorrhages were seen in 21 cases (5 subdural, 16 parenchymal). Cerebral edema was present in 16 cases, and focal necrosis, gliosis and spongiosis in 9 cases (7). In contrast, no histomorphological alteration attributable to EHEC was found in the brains of the five adult patients reported here—in particular, no edema, thrombotic microangiopathy or hemorrhages. The cause of death in the adult patients was diagnosed to be toxic heart failure in conjunction with HUS.

Previous immunohistochemical and biochemical studies have suggested that the localization of CD77/Gb3 in the cell membrane differs between pediatric and adult patients, which may explain—at least in part—why children suffer more frequently from EHEC-associated HUS than adults. In children, CD77 was found in lipid rafts of glomeruli endothelia, whereas it was present

Table 4. Neuropathological findings and immunohistochemistry in brains of enterohemorrhagic *Escherichia coli* (EHEC) patients and controls brain weight in g determined after fixation in formalin; edema evaluated semiquantitatively in 4 grades: 0 = none, 1 = slight, 2 = moderate, 3 = strong; numbers in the header indicate location, 1 = thalamus, 2 = brain stem; numbers in the table indicate staining intensities, 0 = negative, 1 = slight, 2 = moderate, 3 = strong.

Abbreviations: GFAP = glial fibrillary acidic protein; IBA-1 = ionized calcium-binding adapter molecule 1; LCA, leukocyte common antigen; TNF-α = tumor necrosis factor-α; VCAM = vascular cell adhesion molecule-1; VEGF = vascular endothelial growth factor; TNF-α = tumor necrosis factor-α..

Patient	Brain weight	Brain swelling	Neuropathological findings	TNF-α		GFAP		Vimentin		LCA		HLA-DR		CD77		ZO-1		VEGF		IBA-1		Angio-poietin-1		MAP2c		Nestin		% CD77+ Vessels		% VCAM-1 + Vessels	
				1	2	1	2	1	2	1	2	1	2	1	2	1	2	1	2	1	2	1	2	1	2	1	2	1	2	1	2
EHEC																															
1	1200	None	No pathological alterations	3	3	0	1	0	0	0	0	1	1	3	2	1	3	2	3	3	3	3	3	3	3*	0	0	0.0	7.1	53.94	68.47
2	1263	Slight	No pathological alterations	1	3	0	0	0	0	0	0	1	1	2	1	3	3	2	2	1	1	2	2	3	3	0	0	0.0	5.2	38.16	18.6
3	1200	Slight	Old infarctions, aneurysm of the communicating anterior artery	2	3	0	0	1	0	0	0	1	0	3	3	1	3	2	2	2	3	3	3	3	3*	0	0	55.8	15.4	13.4	15.2
4	1396	Moderate	No pathological alterations	1	2	0	0	0	0	0	0	1	1	2	3	3	3	3	3	3	3	3	3	3	3	0	0	69.2	19.2	91.46	9.1
5	1649	Slight	Fresh hypoxic ischemic damage in the hippocampus after resuscitation	2	3	0	0	0	0	0	0	0	0	3	3	3	3	2	2	2	2	3	3	2	3	0	0	1.4	0.0	78.15	31.48
Controls																															
6	1225	Slight	No pathological alterations	1	1	1	1	0	0	0	1	0	1	0	0	1	0	2	2	0	0	1	1	2	2	0	1	0.0	0.0	1.0	12.5
7	1386	Slight	Senile plaques, Rathke cyst	3	3	0	0	0	0	1	1	1	1	1	2	3	3	2	3	1	2	3	3	3	3	0	0	7.5	7.4	39.21	5.26
8	1295	Slight	Old fronto-basal contusion	2	2	1	0	0	0	0	0	0	0	1	0	1	—	—	2	1	—	3	3	3	3	0	0	0.0	—	0.0	5.4
9	1270	Slight	Hypertensive microangiopathy with cortical and subcortical necroses	1	2	2	0	1	1	0	0	0	0	3	3	3	3	3	3	2	2	3	3	2	3	0	0	79.0	69.0	2.85	75.0
10	1276	None	Senile plaques, amyloid angiopathy	2	3	1	1	0	0	0	0	1	0	0	2	3	—	3	2	3	3	3	1	3	3	0	0	16.7	0.0	43.07	—

*Demonstration of axonal swellings; CD34 labeled the endothelia in all cases, labeling of activated caspase 3 was negative in all EHEC cases (controls not investigated), no increased amounts of von Willebrand factor and no thrombus formation was found in EHEC and control samples, no clear difference of LAMP-1 expression in neurons, endothelia and neuropil in EHEC and control cases.

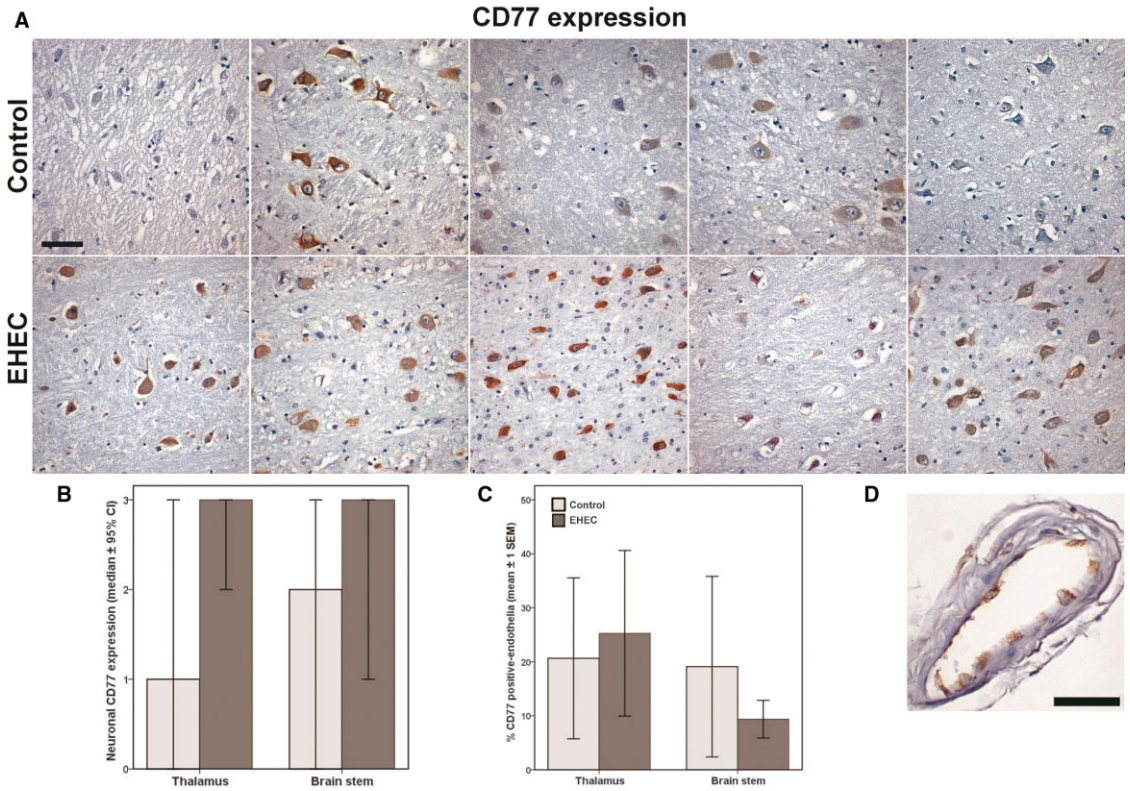

Figure 4. Neuronal and endothelial CD77 expression in the brain of enterohemorrhagic *Escherichia coli* (EHEC) patients and controls. A. CD77 immunohistochemistry of thalamus samples of all 10 cases demonstrating increased CD77 expression in EHEC cases in the second row compared with controls in the first row, counter stain hemalum. Scale bar: 50 μm. B. Median expression levels of CD77 in thalamus and brain stem of controls and EHEC patients, median values of semiquantitative evaluation ± 95% confidence intervals. C. Percent of vessels with endothelial expression of CD77 in a randomly chosen area of 9 mm^2 ± 1 standard error of the mean. D. Example of a vessel with CD77-positive endothelia, counter stain hemalum. Scale bar: 50 μm.

in the detergent-soluble membrane fraction in adults (8). Studies by Mizuguchi *et al* (15) suggested that the age-dependent cell membrane localization of CD77 may also apply for endothelia in the central nervous system (CNS). The authors found that intravenous application of Stx2 in rabbits led to neurological symptoms at lower doses in young animals than in adults, and vascular lesions such as swelling of the endothelial cells and karyorrhexis of medial cells were specific to the CNS of young animals. It has been demonstrated by several groups that CD77 located in lipid rafts is subject to endocytosis and subsequent transport to the endoplasmic reticulum (ER) via the Golgi apparatus, whereas CD77 present in the detergent-soluble membrane fraction is trafficked to lysosomes (5, 9, 21). Interestingly, intracellular transport and processing of Stx depends on the presence of the Golgi protein GPP130 and degradation of GPP130 by increased concentrations of manganese leads to lysosomal processing of Stx resulting in protection against Stx toxicity in cell culture and in mice (16). Lysosomal degradation was found to be the predominant way of toxin processing in monocytes and macrophages and was associated with expression of interleukin-1 (IL-1), IL-1β and TNF-α suggestive for activation of neuroinflammation (20).

In contrast, in cells where CD77 resides in lipid rafts, the toxin is enzymatically cleaved in the ER, resulting in a catalytically active toxin fragment that inactivates 28S rRNA ribosomal subunits in the cytosol. The ribotoxic stress triggers apoptosis via caspase and mitochondrial-dependent signaling (22).

In the present study, no signs of apoptosis were found in endothelia or neurons, neither in standard stains nor by immunohistochemical labeling of activated caspase 3 arguing against ribotoxic stress. Instead, immunofluorescence and Western blot studies revealed an increased expression of IL-1β and its precursor in neurons of the frontal cortex. Synthesis of IL-1β precursor was previously shown to be initiated by Toll-like receptor agonists such as endotoxins (4). Furthermore, a mild inflammatory response characterized by slight increase of IBA-1 positive microglia and an increased IBA-1 expression in Western blotting was found in the EHEC patients in our study. The absence of ribotoxic stress in conjunction with activation of neuroinflammation speaks in favor of a lysosomal inactivation of Stx in adults EHEC patients. To follow this hypothesis further, we investigated the expression of LAMP-1, which, however, showed no differences in EHEC cases and controls in vessels and neurons in EHEC cases and controls. Animal studies with defined conditions may help to clarify this matter.

For Stx, the toxic injury of a vulnerable organ is a direct function of its dose. Hence, if the toxin primarily and mainly binds to

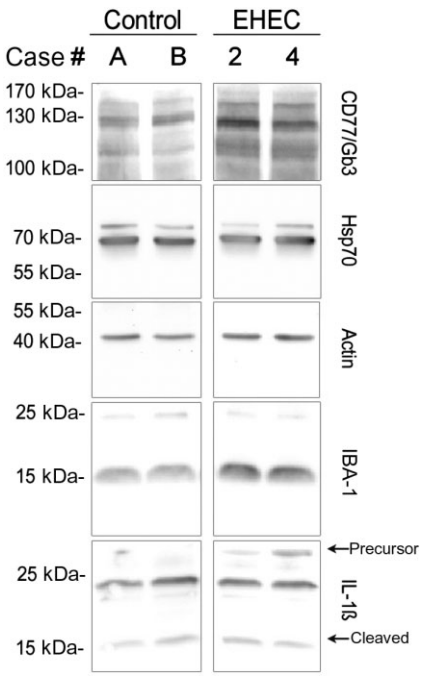

Figure 5. Immunoblots of CD77, Hsp70, actin, IBA-1 and IL-1β. Western blot analyses of frontal cortex of EHEC patients compared with controls using antibodies against CD77/Gb3, Hsp70 IBA-1 and the mature (cleaved) and precursor forms of IL-1β. Actin is shown as loading control and sizes of marker is indicated in kDa. Elevated steady-state levels in homogenates of frontal cortex of EHEC patients compared with controls.

resistant cells, the susceptible organs may be protected from toxic effects. This point has been put forward to explain why some people suffer from a complicated course of EHEC infection and others do not. CD77/Gb3 is also a blood group antigen in P/P1/Pk-related blood group phenotypes. P1 individuals (80% of Caucasians) express P/globotetraosylceramide (Gb4), P1 and Pk/Gb3 antigens on the cell surface, whereas P2 individuals (20% of Caucasians) show P/Gb4 expression and only very low levels of Pk/Gb3. Rarely individuals are deficient of one or more P-blood group antigens (no expression of P/Gb4 in 1 in 5 million people; lack of P/P1/Pk antigens in 1 in 1 million people) (2). It has been proposed that individuals who express significant amounts of Pk/Gb3 on their erythrocytes may be less prone to a complicated course of EHEC infection because Stx is absorbed before reaching the target cells in the kidney or brain. In accordance with this assumption, no or only a weak agglutination of erythrocytes by anti-P antiserum was found in patients who had a complicated course of an infection with *E. coli* O157 (82.4% of patients who developed a thrombotic microangiopathy and 83.3% of patients suffering from HUS; *E. coli* O157 outbreak in Scotland in 1996, n = 186) (1).

The view that high levels of CD77/Gb3 protect the organism from the toxic effects of Stx is further supported by two other studies. Lack of a-galactosidase A (a-GalA), the underlying defect in Fabry disease, leads to massive accumulation of CD77/Gb3. CD77/Gb3-overexpressing a-GalA-knockout mice are protected against lethal intraperitoneal doses of Stx2 (3). The authors hypothesized that excess amounts of Gb3 may reduce toxin delivery to susceptible tissues. And indeed, Neri *et al* (18) could demonstrate that monovalent Stx ligands of phosphatidylethanolamine dipalmitoyl-Gb3 (Gb3-PEDP) and galabiosyl (Gb2)-PEDP strongly neutralized the cytotoxicity of Stx *in vitro*.

In our cohort of EHEC patients, immunohistochemistry of thalamus and brain stem samples as well as Western blot analyses of frontal cortex demonstrated increased expression of CD77. The increased CD77 expression cannot be attributed to HUS or septicemia as there was no association of CD77 expression with clinical parameters such as serum levels of urea, C-reactive protein (CRP) or leucocyte counts. It is tempting to speculate that the high levels of CD77 are a direct response to Stx exposure in an effort to limit toxic effects. This is in line with an animal study showing that intracerebroventricular administration of Stx2 in rat brains is associated with significantly increased levels of CD77/Gb3 in neurons (23). Further studies to investigate CD77/Gb3 expression on neurons in EHEC patients without neurological symptoms would help to clarify this matter.

Correlational analysis of all cases (EHEC plus controls) revealed an association between the number of CD77-positive vessels and VEGF expression in neurons. VEGF expression in normal brain is found in neurons and the choroid plexus and is thought to function in endothelial survival and maintenance and it is not associated with blood–brain barrier breakdown or angiogenesis per se (14). VEGF has also direct neuroprotective effects in hypoxia and is upregulated in neurons after stroke (14). Hitherto, VEGF expression has been linked to CD77 only in Fabry disease where endothelial cells are a preferential target of CD77/Gb3 storage. It was found that VEGF-A serum levels were significantly higher in Fabry patients than in controls. VEGF-A levels also correlated with renal and neurological manifestations in Fabry patients (24). The authors suggested that the rise of VEGF-A levels may develop in response to the vascular damage, which occurs in this lysosomal disorder (24). In the patients presented here, a damage of the vasculature was not detected by light and electron microscopy, and CD77/Gb3 expression in vessels was not associated with EHEC. In addition, the association of endothelial CD77 expression with VEGF expression in neurons was independent of EHEC.

In conclusion, the neuropathological post-mortem examination of five brains of adult EHEC patients with HUS and neurological symptoms showed no classical vascular changes such as hemorrhages or a thrombotic microangiopathy as previously reported in pediatric cohorts. Further, no apoptosis was observed in neurons. However, an increased neuronal expression of CD77/Gb3 and activation of neuroinflammation suggested at least a transient exposure of the brain parenchyma to Shiga toxin. The lack of endothelial and neuronal injury may indicate a detoxification of Stx in lysosomes in the brain of adult patients similar to the toxin processing in monocytes.

ACKNOWLEDGMENTS

We are grateful to Mrs. K. Richter for excellent technical assistance.

DECLARATION

This is to confirm that no work resembling the enclosed article has been published or is being submitted for publication elsewhere. We certify that we have each made a substantial contribution so as to qualify for authorship. The authors declare that they have no conflicts of interest.

REFERENCES

1. Blackwell CC, Dundas S, James VS, Mackenzie DA, Braun JM, Alkout AM *et al* (2002) Blood group and susceptibility to disease caused by *Escherichia coli* O157. *J Infect Dis* **185**:393–396.
2. Branch DR (2010) Blood groups and susceptibility to virus infection: new developments. *Curr Opin Hematol* **17**:558–564.
3. Cilmi SA, Karalius BJ, Choy W, Smith RN, Butterton JR (2006) Fabry disease in mice protects against lethal disease caused by Shiga toxin-expressing enterohemorrhagic *Escherichia coli*. *J Infect Dis* **194**:1135–1140.
4. Dinarello CA (2005) Blocking IL-1 in systemic inflammation. *J Exp Med* **201**:1355–1359.
5. Falguières T, Mallard F, Baron C, Hanau D, Lingwood C, Goud B *et al* (2001) Targeting of Shiga toxin B-subunit to retrograde transport route in association with detergent-resistant membranes. *Mol Biol Cell* **12**:2453–2468.
6. Fründt TW, Höpker W-W, Hagel C, Sperhake JP, Isenberg AH, Lüth S *et al* (2013) EHEC-0104:H4-Ausbruch im Sommer 2011. *Rechtsmedizin* **23**:374–382.
7. Gallo EG, Gianantonio CA (1995) Extrarenal involvement in diarrhoea-associated haemolytic-uraemic syndrome. *Pediatr Nephrol* **9**:117–119.
8. Khan F, Proulx F, Lingwood CA (2009) Detergent-resistant globotriaosyl ceramide may define verotoxin/glomeruli-restricted hemolytic uremic syndrome pathology. *Kidney Int* **75**:1209–1216.
9. Lingwood CA, Binnington B, Manis A, Branch DR (2010) Globotriaosyl ceramide receptor function—where membrane structure and pathology intersect. *FEBS Lett* **584**:1879–1886.
10. Loos S, Ahlenstiel T, Kranz B, Staude H, Pape L, Härtel C *et al* (2012) An outbreak of Shiga toxin-producing *Escherichia coli* O104:H4 hemolytic uremic syndrome in Germany: presentation and short-term outcome in children. *Clin Infect Dis* **55**:753–759.
11. Löbel U, Eckert B, Simova O, Meier-Cillien M, Kluge S, Gerloff C *et al* (2014) Cerebral magnetic resonance imaging findings in adults with haemolytic uraemic syndrome following an infection with *Escherichia coli*, subtype O104:H4. *Clin Neuroradiol* **24**:111–119.
12. Magnus T, Röther J, Simova O, Meier-Cillien M, Repenthin J, Möller F *et al* (2012) The neurological syndrome in adults during the 2011 northern German *E. coli* serotype O104:H4 outbreak. *Brain* **135**:1850–1859.
13. Mayer CL, Leibowitz CS, Kurosawa S, Stearns-Kurosawa DJ (2012) Shiga toxins and the pathophysiology of hemolytic uremic syndrome in humans and animals. *Toxins (Basel)* **4**:1261–1287.
14. Merrill MJ, Oldfield EH (2005) A reassessment of vascular endothelial growth factor in central nervous system pathology. *J Neurosurg* **103**:853–868.
15. Mizuguchi M, Sugatani J, Maeda T, Momoi T, Arima K, Takashima S *et al* (2001) Cerebrovascular damage in young rabbits after intravenous administration of Shiga toxin 2. *Acta Neuropathol* **102**:306–312.
16. Mukhopadhyay S, Linstedt AD (2012) Manganese blocks intracellular trafficking of Shiga toxin and protects against Shiga toxicosis. *Science* **335**:332–335.
17. Nathanson S, Kwon T, Elmaleh M, Charbit M, Launay EA, Harambat J *et al* (2010) Acute neurological involvement in diarrhea-associated hemolytic uremic syndrome. *Clin J Am Soc Nephrol* **5**:1218–1228.
18. Neri P, Tokoro S, Yokoyama S, Miura T, Murata T, Nishida Y *et al* (2007) Monovalent Gb3-/Gb2-derivatives conjugated with a phosphatidyl residue: a novel class of Shiga toxin-neutralizing agent. *Biol Pharm Bull* **30**:1697–1701.
19. Rohde H, Qin J, Cui Y, Li D, Loman NJ, Hentschke M *et al* (2011) Open-source genomic analysis of Shiga-toxin-producing *E. coli* O104:H4. *N Engl J Med* **365**:718–724.
20. Shimada O, Ishikawa H, Tosaka-Shimada H, Atsumi S (1999) Exocytotic secretion of toxins from macrophages infected with *Escherichia coli* O157. *Cell Struct Funct* **24**:247–253.
21. Smith DC, Sillence DJ, Falguières T, Jarvis RM, Johannes L, Lord JM *et al* (2006) The association of Shiga-like toxin with detergent-resistant membranes is modulated by glucosylceramide and is an essential requirement in the endoplasmic reticulum for a cytotoxic effect. *Mol Biol Cell* **17**:1375–1387.
22. Tesh VL (2012) Activation of cell stress response pathways by Shiga toxins. *Cell Microbiol* **14**:1–9.
23. Tironi-Farinati C, Loidl CF, Boccoli J, Parma Y, Fernandez-Miyakawa ME, Goldstein J (2010) Intracerebroventricular Shiga toxin 2 increases the expression of its receptor globotriaosylceramide and causes dendritic abnormalities. *J Neuroimmunol* **222**:48–61.
24. Zampetti A, Gnarra M, Borsini W, Giurdanella F, Antuzzi D, Piras A *et al* (2013) Vascular endothelial growth factor (VEGF-a) in Fabry disease: association with cutaneous and systemic manifestations with vascular involvement. *Cytokine* **61**:933–939.

SUPPORTING INFORMATION

Additional Supporting Information may be found in the online version of this article at the publisher's web-site:

Figure S1. Expression of CD34, vimentin, MAP2c, nestin, LAMP-1 and VCAM-1 in the thalamus and brain stem of EHEC patients and controls.